A Fast Digital Filter Algorithm for Gamma-Ray Spectroscopy With Double-Exponential Decaying Scintillators

H. Tan, M. Momayezi, A. Fallu-Labruyere, Y. X. Chu, and W. K. Warburton, *Member, IEEE*

***Abstract*—Scintillators like CsI(Na), having double-exponential decay times, typically cannot be used in high-count rate applications due to the complicated pulse shapes created by the convolution of their light output decay curves with the decay constant of charge integrating preamplifiers. We present here a novel digital filtering algorithm that is capable of using CsI(Na) at input count rates exceeding 250 kcps, while still achieving good energy resolution. We used a 2.54 cm diameter and 2.54 cm long CsI(Na) crystal, whose scintillation light can be best described by a short component with a 550 ns decay time and a long component with a 4 μs decay time. The crystal was coupled to a 2.86 cm diameter photomultiplier tube. The digital filtering algorithm was implemented in XIA's all-digital Polaris spectrometer, in which five running sums were captured from each digitized scintillation pulse and the Polaris's on-board DSP read these sums and used a set of precomputed coefficients to reconstruct the pulse's total light output as a measure of the deposited energy. The algorithm was tested at different input count rates, ranging from 19 kcps to 270 kcps using a 1 mCi ^{137}Cs source. The energy resolution (full-width at half-maximum) at 662 keV was 10.7% at 19 kcps and 11.7% at 270 kcps with a filter rise time of 1.0 μs, and improved to 7.0% and 8.4%, respectively, with a filter rise time of 3.2 μs. The energy peak shifted by less than 0.3% for input count rates below the maximum throughput point. Output count rates of 65.3 and 17.8 kcps were obtained with filter rise time of 1.0 and 3.2 μs, respectively, at an input count rate of 270 kcps. This algorithm can be easily adapted to other double-exponential decaying scintillators by changing the decay times used in the energy reconstruction formula.**

***Index Terms*—Author, please supply your own keywords or send a blank e-mail to keywords@ieee.org to receive a list of suggested keywords.**

I. INTRODUCTION

SCINTILLATORS have been the earliest and most widely used radiation detectors for gamma-ray spectroscopy due to their high stopping power, which provides efficient detection of high-energy gamma-rays. Traditionally, the scintillation light from these scintillators is measured by a photomultiplier tube (PMT) whose output is fed into a charge integrating preamplifier with a decay constant of approximately 50 μs before being processed by other electronics such as shaping amplifiers [1]. Scintillators such as CsI(Na), CsI(Tl), $Gd_2SiO_5 : Ce$ [2], and YAG:Ce [3], etc., and new scintillators such as $LaCl_3 : Ce^{3+}$ [4], emit scintillation light with more than one exponential decay time. The convolution of the multiple exponential decay times of the scintillation pulse and the preamplifier decay time creates a poorly defined mix of characteristic times, which renders useless the analog spectrometer's traditional pole/zero cancellation and baseline restorer stages. Hence, it is commonly believed that such scintillators cannot be used for gamma-ray spectroscopy with input count rates exceeding 50 kcps.

This paper describes a novel fast digital filter algorithm that is capable of handling double-exponential decaying scintillators for high resolution, high throughput gamma-ray spectroscopy. Implemented as a special multiterm filter on a digital spectrometer, this algorithm was used to process scintillation pulses from a CsI(Na)/PMT detector at input count rates exceeding 270 kcps while achieving excellent energy resolution and system linearity. It can also be easily adapted to other double-exponential decaying scintillators by changing the corresponding decay times.

II. THEORY

Digital gamma-ray spectrometers use various digital filter algorithms such as triangular, trapezoidal [5], [6], or cusp-like [7] filters to process radiation pulses that are directly digitized from outputs of a preamplifier or a simple current-to-voltage converter. A triangular filter, which maps a step-like radiation pulse to a triangular pulse whose amplitude is proportional to the step size, is the simplest digital shaping filter and is good for very fast signals. Where signals have varying rise times due to charge collection time variations or otherwise, trapezoidal filters offer improved ballistic deficit correction and better energy resolution than triangular filters or other shaping methods that do not produce flat-top output pulses [8].

The application of digital trapezoidal shaping to gamma-ray spectroscopy with scintillators takes into account the fact that scintillation pulses decay exponentially. To illustrate the fast digital filter algorithm for double-exponential decaying scintillators, we first introduce the use of digital trapezoidal filtering on single-exponential decaying scintillators. From that, we explain how to derive the new fast digital filter algorithm.

A. Single-Exponential Decaying Scintillators

Fig. 1 shows the response of a digital trapezoidal filter to a scintillation pulse with single-exponential decay time, as it appears when the output of a photomultiplier tube is directly digitized. The pulse arrives at time t_0 with initial amplitude of E_0 and decays exponentially with a time constant τ_1. The signal

Manuscript received November 10, 2003; revised May 15, 2004.

The authors are with X-Ray Instrumentation Associates, Newark, CA 94560 USA (e-mail: htan@xia.com; momayezi@xia.com; anthony@xia.com; yxchu@xia.com; bill@xia.com).

Digital Object Identifier 10.1109/TNS.2004.832984

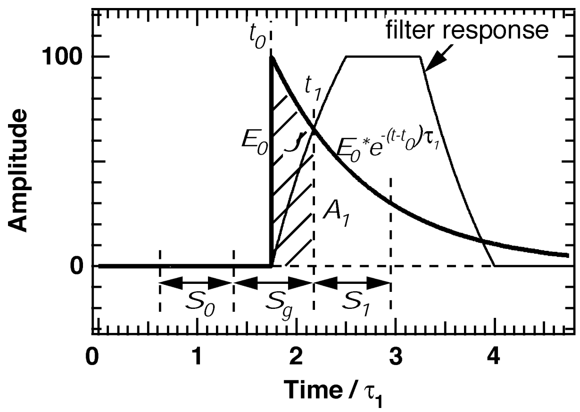

Fig. 1. Illustration of the response of a digital trapezoidal filter to a scintillation pulse with single-exponential decay time τ_1.

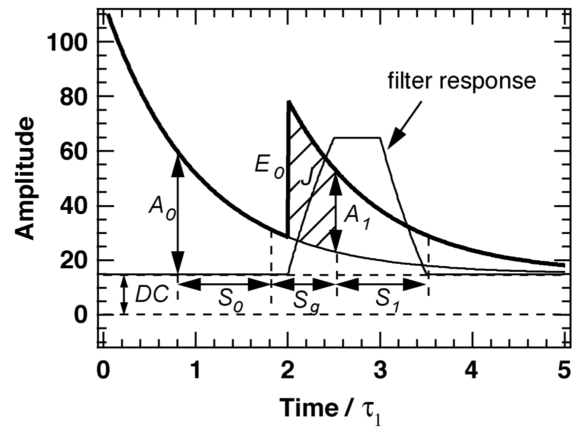

Fig. 2. Construction of a trapezoidal filter for overlapping single-exponential decaying scintillation pulses.

amplitude at time t_1 is A_1, and we define J as the sum of discrete samples between t_0 and t_1.

The primary objective of our filter measurement is to determine the area under the pulse, which is proportional to the energy deposited in the scintillator, without performing a summation to infinite time, which is typically precluded by the arrival of the next pulse at high counting rates. We develop the formalism for doing so as follows. First, referring to Fig. 1, we note that the summation to infinity of the discrete samples is given by

$$\begin{aligned} A_T &= \sum_{i=0}^{\infty} E_i = E_0 r_1 \\ &= \sum_{i=0}^{g} E_i + \sum_{i=g+1}^{\infty} E_i = J + A_1 r_1 \end{aligned} \tag{1}$$

where $i = 0$ corresponds to the first nonzero measurement point, $r_1 = (1 - b_1)^{-1}$, $b_1 = \exp(-\Delta t/\tau_1)$, Δt is the time between samples, and τ_1 is the exponential decay time. In the second part of the equation, we have split the summation into a first part over the region S_g and from there to infinity. A_1 is the value of E at the start of the S_1 region, i.e., time t_1. Equation (1) is true even for pulses that do not have the sharp rising edge shown in Fig. 1, so long as the entire rise time falls within the region S_g. Therefore, in this simple case, if we can use our digital filter to measure both A_1 and J, we can compute an estimate of the full deposited energy, as represented by the total light output. In this derivation, the lengths of S_g and S_1 are arbitrary. In practice, they will be adjusted to optimize the energy resolution, with $S_0 = S_1 = t_p$, the filter peaking time, and $S_g = t_g$, the trapezoidal flat-top.

In practice, scintillation pulses will overlap, i.e., the decaying tails from previous pulses adding to the current pulse, and a DC-offset will be present. Such a pulse is shown in Fig. 2 where DC is the DC-offset, A_0 is the signal amplitude above DC at the start of running sum S_0, A_1 is the second pulse amplitude above the first pulse's tail at the beginning of running sum S_1, and J is the sum of discrete samples of the second pulse in running sum S_g.

To determine A_T for the second pulse, we first express three consecutive running sums S_0, S_g, and S_1 as linear functions of A_0, J, and A_1 (ignoring the DC-offset for the moment). For instance, $S_1 = A_0 \cdot b_1^{(L_0+L_g)} \cdot (1-b_1^{L_1}) \cdot r_1 + A_1 \cdot (1-b_1^{L_1}) \cdot r_1$, where L_0, L_g, and L_1 are the length of the three running sums S_0, S_g, and S_1, respectively. Then, solve for A_0, J, and A_1

$$M_{3\times3} \cdot \begin{pmatrix} A_0 \\ J \\ A_1 \end{pmatrix} = \begin{pmatrix} S_0 \\ S_g \\ S_1 \end{pmatrix} \Rightarrow \begin{pmatrix} A_0 \\ J \\ A_1 \end{pmatrix} = M_{3\times3}^{-1} \cdot \begin{pmatrix} S_0 \\ S_g \\ S_1 \end{pmatrix} \tag{2}$$

where M is the 3×3 coefficients matrix, and M^{-1} is its inverse. Then, A_T can be reconstructed according to (1), by using (2) to express A_1 and J in terms of the running sums S_0, S_g, and S_1 as

$$A_T = a_0 S_0 + a_g S_g + A_1 S_1 \tag{3}$$

where the filter coefficients a_0, a_g, and a_1 are sums of the elements M_{ij}^{-1} in the inverse matrix M^{-1} (for instance, $a_0 = M_{21}^{-1} + r_1 \cdot M_{31}^{-1}$). This digital filter estimates the total area of any pulse that arrives within the time period covered by the running sum S_g and is otherwise zero if there is no DC-offset. This filter response is shown in Fig. 2, where we observe that it looks exactly the same as in Fig. 1, except for a DC-offset. This shows that we are correctly canceling the tails from previous pulses.

Next, we consider the presence of DC-offsets. The filter described by (3) maps an exponentially decaying tail to zero, but is sensitive to the DC-offset, which can be measured in the absence of a pulse. Now the running sums become baseline sums B_0, B_g, and B_1, and the filter response is

$$F_B = a_0 B_0 + a_g B_g + a_1 B_1 = k \cdot \mathrm{DC} \tag{4}$$

where k depends on the running sum lengths, filter constants, and scintillation decay time. Assuming that the DC-offset varies slowly on a time scale set by the filter time, a recent measurement of F_B can make A_T insensitive to a DC-offset

$$F_C = \sum_{i=0,g,1} a_i (S_i - B_i). \tag{5}$$

B. Double-Exponential Decaying Scintillators

The pulse of a double-exponential decaying scintillator can be described as

$$E(t) = E_{01} \cdot e^{-\frac{t}{\tau_1}} + E_{02} \cdot e^{-\frac{t}{\tau_2}} \tag{6}$$

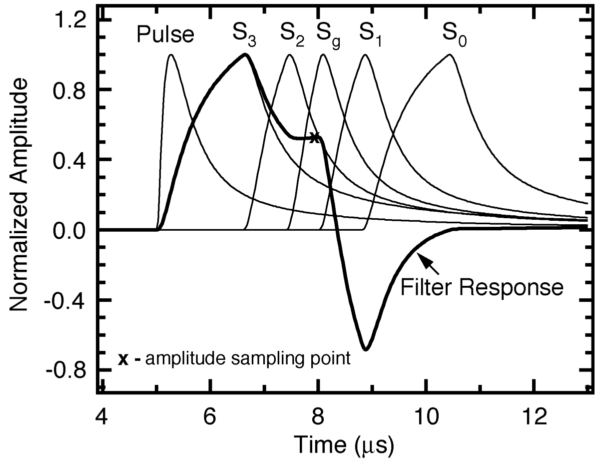

Fig. 3. Digital filter response to a scintillation pulse with double-exponential decay times.

where E_{01} and E_{02} are the initial amplitude of the two decay components, and τ_1 and τ_2 are their corresponding decay time constants. To measure the total energy deposited in such scintillators, a digital filter similar to the one described in (3) can be used, but with five running sums ($S_0 - S_3$ and S_g), since five constants are now required to describe both a pulse and its predecessor. Fig. 3 shows the normalized amplitudes of the scintillation pulse and the five running sums. Similarly to (1), the area under the pulse can be written as

$$\begin{aligned} A_T &= \sum_{i=0}^{\infty} E_i = E_{01} r_1 + E_{02} r_2 \\ &= J + A_{11} r_1 + A_{12} r_2 \end{aligned} \tag{7}$$

where J is the integrated area from the beginning of the pulse to the end of running sum S_g, $r_1 = (1 - \exp(-\Delta t/\tau_1))^{-1}$, $r_2 = (1 - \exp(-\Delta t/\tau_2))^{-1}$, and A_{11} and A_{12} are the two decay components of the signal amplitude at the start of S_2.

For overlapping scintillation pulses, formulae similar to (2) can be derived for the five running sums

$$M_{5\times5} \cdot \begin{pmatrix} A_{01} \\ A_{02} \\ J \\ A_{11} \\ A_{12} \end{pmatrix} = \begin{pmatrix} S_0 \\ S_1 \\ S_g \\ S_2 \\ S_3 \end{pmatrix} \Rightarrow \begin{pmatrix} A_{01} \\ A_{02} \\ J \\ A_{11} \\ A_{12} \end{pmatrix} = M_{5\times5}^{-1} \cdot \begin{pmatrix} S_0 \\ S_1 \\ S_g \\ S_2 \\ S_3 \end{pmatrix} \tag{8}$$

where M is the 5 × 5 coefficients matrix, M^{-1} is its inverse, and the two pairs (A_{01} and A_{02}, A_{11}, and A_{12}) are the two decay components of the signal amplitude similar to A_0 and A_1 as shown in Fig. 2.

Taking into account the presence of DC-offsets, the complete filter for double-exponential decaying scintillators is

$$F_C = \sum_{i=0,1,g,2,3} a_i (S_i - B_i) \tag{9}$$

where B_k ($k = 0, 1, g, 2, 3$) are baseline measurements and a_k ($k = 0, 1, g, 2, 3$) are the coefficients derived from the inverse matrix. Fig. 3 shows the calculated filter response, where the "flat top" of the filter in Fig. 2 has become a "flat ledge" in the middle of the filter response. Over the width of the S_g running sum, this ledge is flat to one part in 10^4 or better. Capturing a value at any point on the ledge therefore produces an accurate estimate of the area under the scintillator light output curve. We note that this ledge commences exactly $S_2 + S_3$ after time t_0. Therefore, if we detect t_0 using a fast (e.g., 100 ns peaking time) triangular filter and discriminator and then capture the five-term energy filter output at a time $T_S = S_2 + S_3 + S_g/2$ later, we will obtain an energy estimate that is insensitive to time jitter in the pulse detection system. This point is marked with an "x" in Fig. 3. In practice, the lengths of the running sums $S_0 - S_3$ and S_g will be adjusted for best energy resolution and/or throughput, just as the single "peaking time" parameter is adjusted in simple trapezoidal filters.

III. Algorithm Implementation

The fast digital filter algorithm described in Section II was implemented in our all-digital high-throughput Polaris spectrometer. The Polaris features a 14-bit ADC sampling at 40 MHz that digitizes the PMT output after some analog conditioning and sends the data stream to a real-time processing unit (RTPU) where the digital trapezoidal filter is applied together with pileup inspection. The final data processing takes place in the on-board digital signal processor (DSP) where the pulse height is reconstructed and binned into a histogram.

We chose the double-exponential decaying scintillator CsI(Na) to exercise the algorithm. A double-exponential decaying model was created for the CsI(Na) light output. From an average of 1000 waveforms acquired using the Polaris (this normalized average pulse was shown in Fig. 3), it was found that the scintillation light was best described by a short component with a 550 ns decay time and a long component with a 4 μs decay time. Taking these two components into account, five running sums of the digitized scintillation pulse were acquired each time the RTPU detects a pulse. At a time T_S after each detected pulse, the DSP read these five sums from the RTPU and reconstructed the pulse height using the coefficients a_k. The running sum lengths were set as follows: $S_1 = S_2 = 0.8\ \mu$s and $S_g = 0.6\ \mu$s, while the lengths of S_0 and S_3 were set to be equal and varied between 1.0 and 3.2 μs. The values of S_1 and S_2 are approximately twice the scintillator's short decay time. Modeling showed that making these times longer did not improve energy resolution significantly, while shortening them does little to increase throughput, which is principally set by the much longer S_0. The length of S_0 or S_3 was called the filter rise time for the convenience of the discussions in Section V. The overall system dead time (T_D) was estimated to be approximately twice the sum of the lengths S_0, S_1, and S_g. The standard extending dead time formula given below describes the relationship between input count rate (ICR), output count rate (OCR) and system dead time T_D [9]:

$$\mathrm{OCR} = \mathrm{ICR} \cdot e^{(-\mathrm{ICR} * T_D)}. \tag{10}$$

As the effectiveness of the algorithm depends on the accuracy of CsI(Na)'s two decay times, it is essential that the CsI(Na) scintillation pulse shape does not change significantly as the incident gamma-ray energy varies. Fig. 4 shows the averaged pulse shapes of CsI(Na) irradiated by gamma-rays from ^{137}Cs

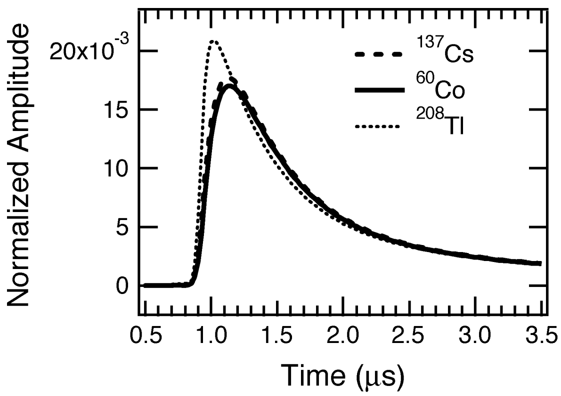

Fig. 4. Averaged pulse shapes of CsI(Na) irradiated by different gamma-ray energies.

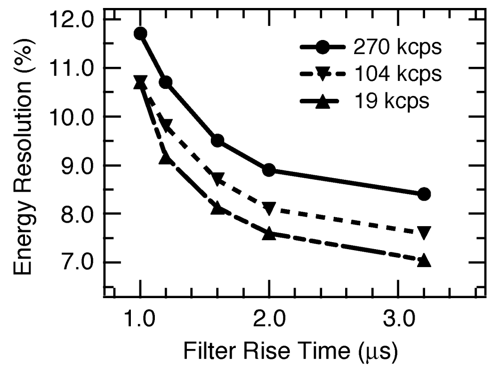

Fig. 5. Energy resolution as a function of filter rise time at different input count rates using a ^{137}Cs source.

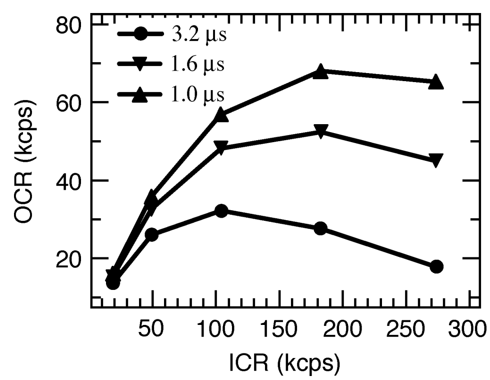

Fig. 6. Output count rate versus input count rate at different filter rise time using a ^{137}Cs source.

(662 keV), ^{60}Co (1173.2 and 1332.5 keV), and ^{208}Tl (2615 keV). The amplitudes were normalized such that the integral over the entire pulse is unity. The ^{208}Tl pulse rise time differed slightly from the ^{60}Co or ^{137}Cs pulse rise times, but the decay times and the ratio of scintillation light contained in the fast to the slow components showed little change for these different gamma-ray energies.

IV. Experimental Measurements

The fast digital filter algorithm was tested for energy resolution, throughput and system linearity at different input count rates and filter rise times. A 2.54 cm diameter and 2.54 cm long CsI(Na) crystal (PhotoPeak, Inc.) was sealed in an aluminum can with one of its flat surfaces coupled to a 2.86 cm diameter PMT with a bi-alkali photocathode (PMT Model R6095 and base Model E990-08, Hamamatsu) using optical grease couplant (Dow Corning, Q2-3067). The PMT output was fed to a current-to-voltage converter that preserved the timing profile of the CsI(Na) scintillation pulses. Its output was connected in turn to the Polaris. A 1 mCi ^{137}Cs source was used to irradiate the CsI(Na) crysta, l and various input count rates were obtained by changing the distance between the source and the crystal.

We also compared the performance of the five-term fast filter to a trapezoidal filter and a semi-Gaussian shaper. In those experiments, we implemented both the digital trapezoidal filter and the five-term fast filter in the Polaris spectrometer, and used a Tennelec TC 244 amplifier for the semi-Gaussian shaper, connecting its unipolar output to a Nucleus Personal Computer Analyzer (PCA-II) card (The Nucleus, Inc.). The PMT output was directly connected to the Tennelec amplifier or the Polaris via the current-to-voltage converter.

V. Results and Discussion

Fig. 5 shows the energy resolution (full-width at half-maximum) for 662 keV gamma-rays from ^{137}Cs at different input count rates. The energy resolution improves as the filter rise time increases at all three input count rates. It was 10.7% at 19 kcps and 11.7% at 270 kcps with a filter rise time of 1.0 μs, and improved to 7.0% and 8.4%, respectively, with a rise time of 3.2 μs. This is because larger fractions of the CsI(Na) scintillation pulse are integrated for longer filter rise times, which in turn reduces the effect of photon statistical fluctuations and also makes the baseline measurements more accurate. The 7.0% figure is very good for CsI(Na) scintillators when processed with standard commercial electronics at low count rates. At a fixed filter rise time, energy resolution also slowly worsens with increasing input count rate, the degradation being more pronounced as the filter rise time increases. The main reason for resolution loss is undetected pileups between large and small energy gamma-rays. In this case, 33 keV Ba K_α X-rays presented the biggest problem.

Fig. 6 shows output count rate as a function of input count rate at three different filter rise times: 1.0, 1.6, and 3.2 μs. Based on their pileup inspection periods, we expect to obtain dead times of 4.8, 6.0, and 9.2 μs for the filters having rise times of 1.0, 1.6, and 3.2 μs, respectively. It is interesting to note that the algorithm performed remarkably well when ICR went far beyond the maximum throughput point, i.e., ICR $= 1/T_D$. For example, at filter rise time of 3.2 μs, the energy resolution rose from 7.0% at 19 kcps to 8.4% kcps at 270 kcps, a change of only 20% even though the max ICR (270 kcps) exceeded $1/T_D$ ($\sim$109 kcps) by a factor of more than 2.

Fig. 7 shows ^{137}Cs 662 keV peak position drift versus input count rate at a filter rise time of 3.2 μs. The energy peak shift was less than 1% over the entire input count rate range, and less than 0.3% for ICR below the maximum throughput point. This shows that the PMT remained in its linear operating range event at the highest count rate.

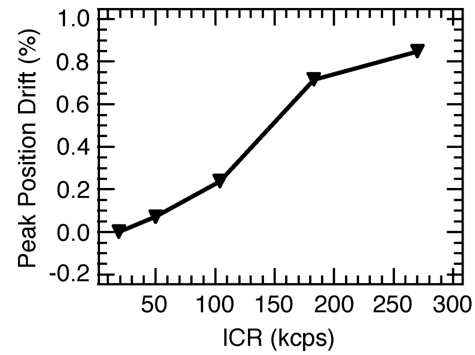

Fig. 7. ^{137}Cs 662 keV peak position drift as a function of input count rate at a filter rise time of 3.2 μs.

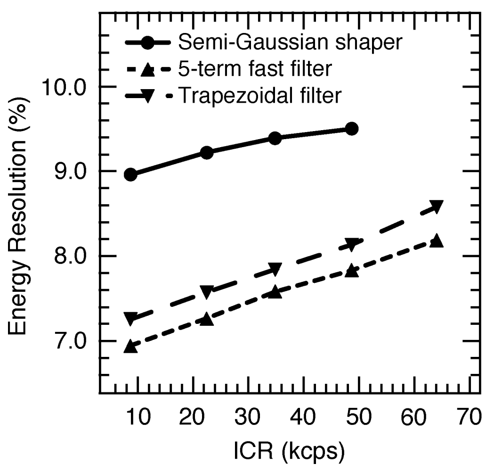

Fig. 8. Comparison of energy resolution for ^{137}Cs 662 keV peak obtained using a semi-Gaussian shaper, a digital trapezoidal filter, or the five-term fast filter.

Fig. 8 compares energy resolution as a function of input count rate for the semi-Gaussian shaper, digital trapezoidal filter, and the five-term fast filter. To have a fair comparison, we made these three filters have approximately the same peaking time by setting the semi-Gaussian shaper's peaking time to 4 μs, the trapezoidal filter's rise time to 4 μs and flat top to 0.6 μs, and the five-term filter's rise time to 3.2 μs. Fig. 8 shows the superiority of the five-term fast filter compared to the digital trapezoidal filter and particularly to the semi-Gaussian shaper. Specifically, the energy resolutions of the five-term filter and the trapezoidal filter degrade slowly as input count rate increases with the five-term filter consistently having better energy resolution than the trapezoidal filter. The semi-Gaussian filter shows much worse energy resolution.

VI. Conclusion

A fast digital filter algorithm was proposed, implemented, and tested for gamma-ray spectroscopy of double-exponential decaying scintillators. It was based on a novel five running sums filter algorithm that is capable of handling slow decaying scintillators like CsI(Na) at ultra-high input count rates while achieving high throughput and good energy resolution. Energy resolutions of 7.0% and 8.4% at 662 keV of ^{137}Cs were obtained at input count rates of 19 and 270 kcps, respectively, for a filter rise time of 3.2 μs, while the output count rate decreases as the filter rise time increases. The digital algorithm reconstructed the energy, taking into account the presence of a fast and a slow component in the scintillation light, making it customizable for other types of double-exponential decaying scintillators as well. It also demonstrated the flexibility of the XIA Polaris spectrometer in dealing with uncommon pulse shapes. Comparison of the energy resolutions obtained using the five-term fast filter, a semi-Gaussian shaper and a trapezoidal filter showed the advantage of the five-term filter over two other types of shaper or filter.

Acknowledgment

The authors appreciate the help and support from I-Yang Lee (Lawrence Berkeley National Laboratory) who made possible the very high count rate measurements.

References

[1] G. F. Knoll, *Radiation Detection and Measurement*, 3rd ed. New York: Wiley, 2000, p. 620.

[2] M. Tanaka, K. Hara, S. Kim, K. Kondo, H. Takano, M. Kobayashi, H. Ishibashi, K. Kurashige, K. Susa, and M. Ishii, "Applications of cerium-doped gadolinium silicate $Gd_2SiO_5 : Ce$ scintillator to calorimeters in high-radiation environment," *Nucl. Instrum. Methods*, vol. A404, pp. 283–294, 1998.

[3] M. Moszyski, T. Ludziejewski, D. Wolski, W. Klamra, and L. O. Norlin, "Properties of the YAG:Ce scintillator," *Nucl. Instrum. Methods*, vol. A345, pp. 461–467, 1994.

[4] E. V. D. van Loef, P. Dorenbos, C. W. E. van Eijk, K. Krämer, and H. U. Güdel, "Scintillation properties of $LaCl_3 : Ce^{3+}$ crystals: fast, efficient, and high-energy resolution scintillators," *IEEE Trans. Nucl. Sci.*, vol. 48, pp. 341–345, June 2001.

[5] V. T. Jordanov, G. F. Knoll, A. C. Huber, and J. A. Pantazis, "Digital techniques for real-time pulse shaping in radiation measurements," *Nucl. Instrum. Methods*, vol. A353, pp. 261–264, 1994.

[6] W. K. Warburton, M. Momayezi, P. Grudberg, and W. Skulski, "Digital pulse processing: New possibilities in portable electronics," *J. Radio. Nucl. Chem.*, vol. 248, no. 2, pp. 301–307, 2001.

[7] V. T. Jordanov and G. F. Knoll, "Digital synthesis of pulse shapes in real time for high resolution radiation spectroscopy," *Nucl. Instrum. Methods*, vol. A345, pp. 337–345, 1994.

[8] V. Radeka, "Trapezoidal filtering of signals from large germanium detectors at high rates," *IEEE Trans. Nucl. Sci.*, vol. 19, pp. 412–428, 1972.

[9] G. F. Knoll, *Radiation Detection and Measurement*, 3rd ed. New York: Wiley, 2000, p. 121.